The Cosmic Ray Mass Composition in the Energy Range $10^{15} - 10^{18}$ eV measured with the Tunka Array: Results and Perspectives

V.V. Prosin[a] * for the Tunka Collaboration:

N.M. Budnev[b], O.A. Chvalaiev[b], O.A. Gress[b], N.N. Kalmykov[a], V.A. Kozhin[a], E.E. Korosteleva[a], L.A. Kuzmichev[a], B.K. Lubsandorzhiev[c], R.R. Mirgazov[b], G. Navarra[d], M.I. Panasyuk[a], L.V. Pankov[b], V.V. Prosin[a], V.S. Ptuskin[e], Yu.A. Semeney[b], B.A. Shaibonov (junior)[c], A.A. Silaev[a], A.A. Silaev (junior)[a], A.V. Skurikhin[a], C. Spiering[f], R. Wischnewski[f], I.V. Yashin[a], A.V. Zablotsky[a], A.V. Zagorodnikov[b]

[a]Skobeltsyn Institute of Nuclear Physics, Moscow State University, Russia

[b]Institute of Applied Physics, Irkutsk State University, Irkutsk, Russia

[c]Institute of Nuclear Research, Russian Academy of Sciences, Moscow, Russia

[d]Dipartimento di Fisica Generale dell'Universita' and INFN, Torino, Italy

[e]Institute of Terrestrial Magnetism, Ionosphere and Radio Wave Propagation, Russian Academy of Sciences, Moscow, Russia

[f]DESY, Zeuthen, Germany

The final analysis of the Extensive Air Shower (EAS) maximum (X_{max}) depth distribution derived from the data of Tunka-25 atmospheric Cherenkov light array in the energy range $3 \cdot 10^{15} - 3 \cdot 10^{16}$ eV is presented. The perspectives of X_{max} studies with the new Cherenkov light array Tunka-133 of 1 km^2 area, extending the measurements up to 10^{18} eV, are discussed.

1. INTRODUCTION

The study of primary mass composition in the energy range $10^{15} - 10^{18}$ eV is of crucial importance for the understanding of the origin of cosmic rays and of their propagation in the Galaxy. The change from light to heavier composition with growing energy marks the energy limit of cosmic ray acceleration in galactic sources (SN remnants), and of the galactic containment. An opposite change from heavy to light composition at higher energy would testify the transition from galactic to extragalactic sources. Both changes are expected in the energy range of interest in the present investigation.

To study the mean composition we use the relation between the logarithm of mass $\ln A$ and the depth X_{max} of the extensive air shower (EAS) maximum: $< X_{max} > \propto < \ln A >$ – which is well-known from electromagnetic cascade theory. X_{max} is derived for every event from the steepness of the atmospheric Cherenkov light lateral distribution function (LDF). We extend here the simplest method of performing such analysis (i.e. of relating the average $< X_{max} >$ and $< \ln A >$ values) to the more correct one based on the analysis of the whole X_{max} distribution.

We summarize the results of the analysis of the Tunka-25 experiment, based on 25 stations covering an area of 0.1 km^2, and therefore tuned to operate between $3 \cdot 10^{15}$ and $3 \cdot 10^{16}$ eV. Both

quoted methods show the beginning of composition change from light to heavy at energies above 10^{16} eV. To extend the study to higher energies, higher statistics and consequently larger sensitive areas and solid angles are needed. Such an array, Tunka-133 (1 km^2 area) is now under construction close to its predecessor Tunka-25. Last winter the first part of the new array operated for about 270 h during clean moonless nights. The first results and perspectives of the new array are presented.

2. TUNKA-25 FINAL RESULTS

The detailed description of the Tunka-25 experiment and the procedure of primary energy measurement and X_{max} analysis from the LDF steepness is given in [1]. The methods developed for the analysis provided the relative accuracy of energy to be $\sim$15% and the error of X_{max} less than 30 g/cm^2.
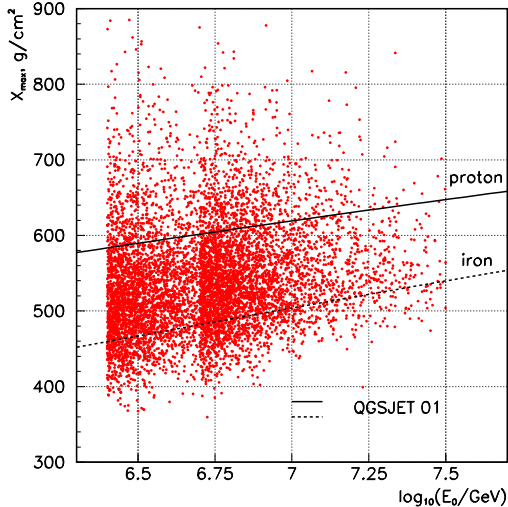

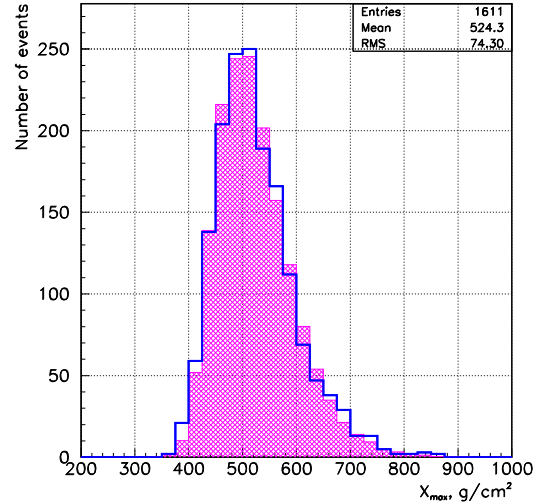Figure 1. Depth of maximum, X_{max}, vs. primary energy E_0 (7632 points).

Figure 2. Depth of maximum, X_{max}, distribution for $6.4 < log_{10}(E_0/GeV) < 6.5$. Line – experiment, filled area – simulation for the complex mass composition containing $\sim$70% of light (p+He) and $\sim$30% of heavy (CNO+iron) nuclei

The experimental plot of the depth of the shower maximum vs. primary energy E_0 is shown in fig. 1. Data points are reported for energy $E_0 > 2.5 \cdot 10^{15}$ eV at zenith angles $\theta \geq 12°$ and for $E_0 > 5 \cdot 10^{15}$ eV at $\theta \geq 25°$. In fact, the analysis of possible distortions of the distribution has shown that no systematic errors are introduced in such energy-angular ranges. The distributions inside narrow logarithmic energy bins (0.1) have been analyzed. The analysis was done as follows. The experimental X_{max} distribution is compared with the simulated one. The simulated distribution is constructed from 4 partial distributions for different nuclei groups – p, He, CNO and Fe. Partial distributions are simulated with a "model of experiment" code assuming the QGSJET-01 model of primary interaction. The code itself includes all the essential parameter correlations and distributions extracted from CORSIKA and takes into account all the apparatus errors and selection

of events. A detailed description of this code is given in [1]. The weight of each group is selected for the best fit of the experimental distribution.

The result for one of the logarithmic bins $(6.4 < log_{10}(E_0/GeV) < 6.5)$ is shown in fig. 2. We note that QGSJET-01 provides the best fit of the left edge of the distribution when compared with the other models. In principle the result of this procedure can give the relative weight of each group of nuclei within the total composition. But limited statistics and the relatively large width of the partial distribution make it almost impossible to distinguish 2 components inside the light (proton+helium) and the heavy (CNO+iron) groups.
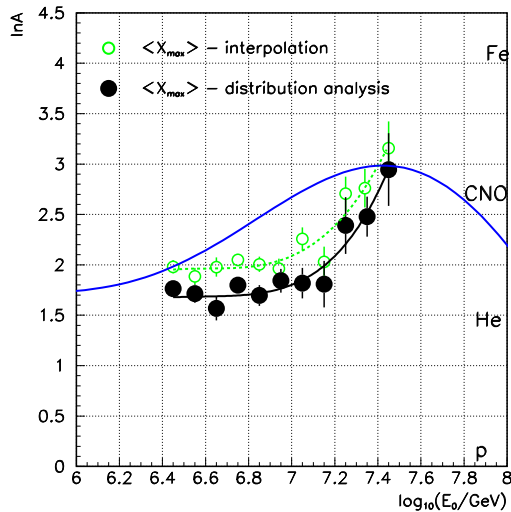

Figure 3. Mean logarithmic mass vs. primary energy. Dense curve is the theory [2], dotted curves are the smoothing approximations of the experimental points.

A more stable solution can be obtained for the percentage of light (p+He) and heavy (CNO+iron) nuclei in the primary composition, that provides a stable estimation of the mean logarithmic mass $< \ln A >$. The obtained experi-

mental dependence of $< \ln A >$ on primary energy E_0 is shown in fig. 3, together with a theoretical curve derived from [2].

One sees that the old method of interpolation shifts $< \ln A >$ systematically by about 0.25 towards heavier composition, compared to the more strict method of the analysis of the full distribution. The mean value obtained with the second method for the knee range of energies $(3 \cdot 10^{15}$ eV) is close to that obtained in the recent balloon experiments for energy about 10 TeV [3]. The rise of $< \ln A >$ for energies above 10^{16} eV is well visible.

3. THE 1 km^2 TUNKA-133 ARRAY

To study the mass composition behavior in the energy range $10^{16}-10^{18}$ eV, the new array Tunka-133 is under construction [4].
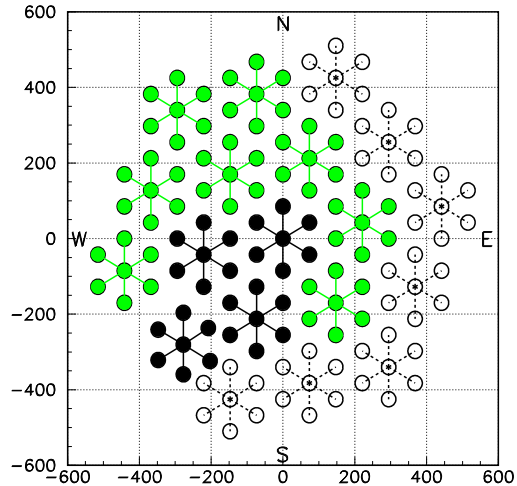

Figure 4. Plan of the Tunka-133 array. Black - 4 clusters operated in winter 2007-2008, grey – 8 clusters ready for operation in winter 2008-2009, open circles – the last 7 clusters to be deployed in 2009.

The array will consist of 133 detectors grouped into 19 clusters each composed of 7 detectors. The map of the array is shown in fig. 4. The new array provides much more information than the previous one. Each detector signal is digitized by an FADC with time step 5 ns. So the waveform of every pulse is recorded, together with the preceding noise, as a total record of 5 μs duration.

The minimal pulse FWHM is about 20 ns and the dynamic range of amplitude measurement about 10^4. The latter is achieved by means of two channels for each detector extracting the signals from the anode and an intermediate dynode of the PMT with different additional amplification factors.

Four clusters operated last winter between November and April. Data have been recorded over 270 hours during clean moonless nights. The average trigger rate was about 0.3 Hz, the number of the registered events was about $3 \cdot 10^5$.

Figure 5. An example of an experimental event. The radii of the circles are proportional to the logarithm of the Cherenkov light flux

4. RECONSTRUCTION OF EAS PARAMETERS.

4.1. Structure of the data processing.

The program of calibration and reconstruction of EAS parameters consists of three main blocks.

1. The first block analyzes the primary data records for each Cherenkov light detector and derives three main parameters of the pulse: front delay at a level 0.25 of the maximum amplitude (t_i), pulse area (Q_i) and full width on half-maximum FWHM$_i$.

2. The second block of codes combines the data of different clusters and provides the relative time and amplitude calibration. Data from various clusters are merged to one event, if the time difference for cluster triggers is less than 2 μs.

The time and amplitude calibration procedure is the same described in [1].

3. The third block of programs reconstructs the EAS core location, primary energy and depth of shower maximum.
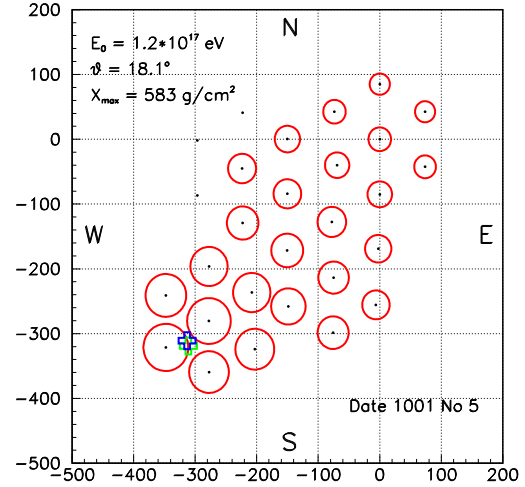
4.2. EAS core reconstruction with the density data Q_i

The first method of EAS core location reconstruction is based on the fitting of the Q_i data by the lateral distribution function (LDF) with varied parameters of steepness (P) and light density at a core distance 175 m (Q_{175}). This function was first suggested by the members of our collaboration in [5], and it is modified here to include large distance measurements: $Q(R) = Q_{kn} f(R)$,

$$f(R) = \begin{cases} \exp\left(\frac{(R_{kn}-R)}{R_0}\left(1 + \frac{3}{R+3}\right)\right), R < R_{kn} \\ \left(\frac{R_{kn}}{R}\right)^{2.2}, \qquad 200 \geq R \geq R_{kn}(1) \\ \left(\frac{R_{kn}}{200}\right)^{2.2}\left(\left(\frac{R}{200}+1\right)/2\right)^{-b}, R > 200 \end{cases}$$

Here R is the core distance (in meters), R_0 is a parameter of the first branch of LDF, R_{kn} is the distance of the first change of LDF, Q_{kn} is the light flux at the distance R_{kn}. The second change occurs at the core distance 200 m, b is the parameter of the third branch. This branch is checked till the distance 700 m with CORSIKA

simulated events. These 4 variables are strictly connected with two main parameters of the LDF – density at 175 m Q_{175} and steepness P:

$$Q_{kn} = Q_{175}(R_{kn}/175)^{-2.2}$$
$$R_0 = \exp(6.79 - 0.564P), \quad (m)$$
$$R_{kn} = 207 - 24.5P, \quad (m)$$
$$b = \begin{cases} 4.84 - 1.23ln(6.5 - P), & P < 6 \\ 3.43, & P \geq 6 \end{cases}$$
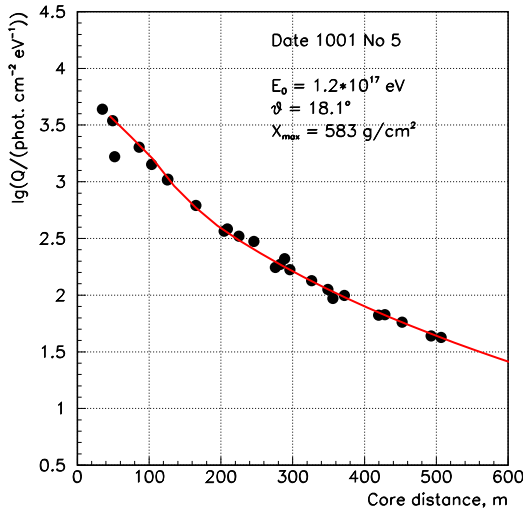

Figure 6. Lateral distribution resulting from fitting the measured light fluxes (points) with the expression (1) (curve) for the event from fig. 5.

4.3. EAS core reconstruction with the pulse widths $FWHM_i$

In addition to the traditional method above described, a new method of EAS reconstruction using Cherenkov light pulse FWHM has been designed and included into the analysis. To fit the experimental $FWHM_i$, the empirical width-distance function (WDF) is used. It has a very simple analytic form (for FWHM > 20 ns and
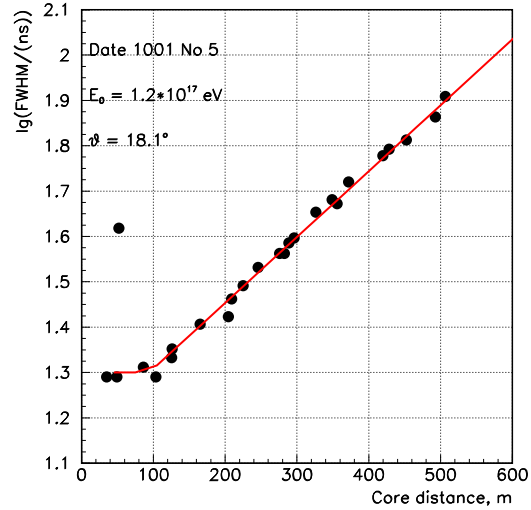

Figure 7. Dependence of Cherenkov light pulse width on the core distance for the event from fig. 5. Points – experiment, line – approximation by expression (2).

$R < 500$ m):

$$\mathrm{FWHM}(R) = 11 \left(\frac{\mathrm{FWHM}(400)}{11} \right)^{\frac{R+100}{500}} ns \qquad (2)$$

FWHM(400) is related to the depth of EAS maximum X_{max}, that will therefore be reconstructed for each event by two independent methods: from the LDF steepness P and the parameter FWHM(400).

An example of a reconstructed shower is presented in fig. 5. The LDF and WDF for this event are shown in fig. 6 and 7, respectively.

5. PERSPECTIVES OF THE PULSE WIDTH ANALYSIS

The absence of FWHM random fluctuations and a simpler expression for the WDF with respect to the LDF one seems to allow us applying the new method of EAS core reconstruction not

only inside, but also outside the array geometry, up to a certain distance.

A similar idea of reconstruction of EAS core distance using pulse width was suggested many years ago by John Linsley [6]. But the use of the idea for charged particle detectors is problematic because of essential random fluctuations of the signal form. Figure 7 shows that in case of Cherenkov light random fluctuations do not play an essential role.

We realize that before using such method of core reconstruction, a detailed study of WDF up to core distances 1000 – 1500 m has to be performed not only with simulation but also experimentally. A positive result of this study would let us expand the sensitive area of the array by $5 - 10$ times compared with the geometrical area covered by the detectors for energies above $5 \cdot 10^{17}$ eV.

Such sensitive area increase will provide $20 - 30$ events with energies above 10^{18} eV during one year (400 h during clear moonless nights) of observation and ensure an overlapping of the Tunka-133 energy range with that of huge installations such as Auger.

6. CONCLUSIONS

1. The analysis of X_{max} distribution obtained with Tunka-25 array provides the mean logarithmic mass of primary cosmic rays. For the energy range $3 \cdot 10^{15} - 10^{16}$ eV it is close to that obtained in balloon experiments for energies around 10^{13} eV and corresponds to a "light" composition $\sim 70\%$ of p+He and $\sim 30\%$ of heavier nuclei. For energies above 10^{16} eV a rapid growth of $< \ln A >$ is observed.

2. The preliminary results obtained with the first stage of the new array Tunka-133 show unique possibilities of the new apparatus recording pulse waveform for each detector. This will provide more reliable measurement of X_{max} with two methods in each individual event.

3. The completion of Tunka-133 with its projected area of 1 km^2, together with the development of the new method of shower core reconstruction from pulse durations, will provide the reliable evaluation of $< \ln A >$ up to 10^{18} eV.

REFERENCES

1. N. M. Budnev et al. (Tunka Collaboration), Proc. 29th ICRC, Pune, India 6 (2005) 257.
2. E.G. Berezhko, H.J. Volk, (2007) arXiv: 0704.1715.
3. A.D. Panov et al. (ATIC Collaboration), Izv. RAS ser. phys., v.72, 3 (2009) to be published.
4. N.M. Budnev et al. (Tunka Collaboration), Proc. 30th ICRC, Merida, Yucatan, Mexico, (2007) arXiv: 0801.3037.
5. EAS-TOP Collaboration and E.E. Korosteleva, L.A. Kuzmichev, V.V. Prosin, Proc. 28th ICRC, Tsukuba, Japan, 1 (2003) 89.
6. J. Linsley, Proc. 19th ICRC. La Jolla. 9 (1985) 434.